Materials Chemistry and Physics 225 (2019) 42–49

Contents lists available at ScienceDirect

Materials Chemistry and Physics

journal homepage: www.elsevier.com/locate/matchemphys

Silver nanoparticles/polydopamine coated polyvinyl alcohol sponge as an effective and recyclable catalyst for reduction of 4-nitrophenol

Mingming Guo, Yunfei Zhang*, Feipeng Du, Yanguang Wu, Qiao Zhang, Can Jiang

School of Materials Science and Engineering, Wuhan Institute of Technology, Wuhan, 430205, China

HIGHLIGHTS

- Silver nanoparticles/polydopamine coated polyvinyl alcohol sponge (AgNPs/D-PVA) composite was prepared and characterized.
- Polyvinyl alcohol sponge incorporated with polydopamine can effectively guarantee the stability and loading amount of AgNPs.
- AgNPs/D-PVA exhibited prominent catalytic activity for the reduction of 4-NP by $NaBH_4$ and can be used as a recyclable catalyst.

GRAPHICAL ABSTRACT

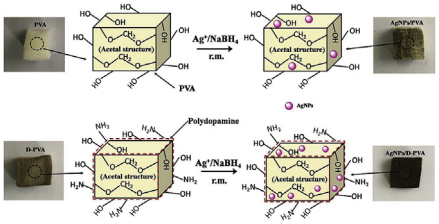

ARTICLE INFO

Keywords:
Polyvinyl alcohol sponge
Silver nanoparticles
Dopamine
Catalysis
4-nitrophenol

ABSTRACT

In this work, silver nanoparticles/polydopamine coated polyvinyl alcohol (AgNPs/D-PVA) sponge were prepared via anchoring silver nanoparticles (AgNPs) on the inner wall of polyvinyl alcohol (PVA) sponge with dopamine as intermediate. The AgNPs/D-PVA were characterized by Fourier transform infrared spectroscopy (FTIR), scanning electron microscopy (SEM), Brunauer-Emmett-Teller (BET) surface area analyzer, X-ray diffraction pattern (XRD), thermogravimetric analysis (TG) and ultraviolet–visible (UV–vis) spectroscopy. The catalytic activity of the AgNPs/D-PVA was evaluated for the reduction of 4-nitrophenol using $NaBH_4$ at room temperature. The coupling effect of dopamine enables AgNPs to be firmly anchored on the inner-wall of PVA sponges. AgNPs/D-PVA exhibits excellent catalytic performance for 4-NP and a good stability up to 4 cycles without a significant loss of its catalytic activity. This work develop a low-cost, high-performance and reusable of AgNPs/D-PVA sponge for the efficient and eco-friendly conversion of toxic 4-nitrophenol into harmless 4-aminophenol, which has potential application in sewage treatment.

1. Introduction

Recently, noble metallic nanoparticles (NPs), such as palladium, gold and silver NPs, have achieved considerable attention for their excellent reactivity and high selectivity towards catalytic degradation of organic pollutants [1–4]. Among them, silver nanoparticles (AgNPs) have been extensively used as catalyst for the reduction of organic dyes because of relatively more abundant resources and lower cost. However, AgNPs are easily susceptible to oxidation and tend to agglomerate because of their high surface energy, leading to a reduction in their catalytic activity [5,6]. One effective way to overcome these problems is to anchor AgNPs on some supports. Up to now, various porous materials such as 2D silica nanosheets [7], fibrous nanosilica [8], nanofibrillated cellulose [9], microporous chitosan [10], chitosan sponge [11,12] and porous carbon nanosheets [13] have been used as matrix for loading AgNPs. Noticeably, polymer porous materials, especially recyclable and nontoxic biopolymer matrix as the supports for AgNPs catalyst have attracted remarkable attention [14–17]. Zhao et al.

* Corresponding author.
E-mail address: zyf3006@126.com (Y. Zhang).

https://doi.org/10.1016/j.matchemphys.2018.12.049
Received 3 October 2018; Received in revised form 6 December 2018; Accepted 19 December 2018
Available online 20 December 2018
0254-0584/

prepared alginate/AgNPs fibers via in-situ reduction of Ag^+-alginate fibers [14]. Alshehri et al. prepared chitosan/AgNPs/multi-walled carbon nanotubes (MWCNTs) composites through depositing AgNPs onto carboxyl-functionalized MWCNTs (Ag@MWCNTs) and combining Ag@MWCNTs with chitosan polymer matrix [15]. Mao et al. reported on the in-situ synthesis of AgNPs onto the surface of polyacrylamide/polypyrrole/graphene oxide nanosheets composite [16]. Liang et al. have provided a facile and robust method to anchor AgNPs on amino-modified cellulose paper [17]. It is worth noting that Liang et al. proved that amino group ($-NH_2$) was able to provide stable anchoring centers for silver ions due to lone pair of electrons of $-NH_2$ for binding metal ions through an electron pair sharing [17]. Therefore, ideal candidates to anchor AgNPs are still highly desired.

Dopamine is a mimic of mussel protein, which can be polymerized into polydopamine (PDA) under a weak alkaline environment at room temperature [18]. Recently, PDA has attracted intensively research interesting in the synthesis of noble metal NPs (AuNPs, AgNPs, etc) catalysts for two reasons [19–22]. For one reason, PDA contains abundant functional groups, such as catechol, amine, and imine, which can serve as the anchors for the loading of noble metal ions. PDA can reduce noble metal salt into metal NPs by virtue of its powerful reducing capacity [23]. For another reason, PDA can also be used as binding agents, which help stabilize the produced NPs [24]. In addition, PDA can be easily deposited on virtually all types of inorganic and organic substrates [25–27]. Therefore, PDA has opened an effective route to modify various substrates for loading more metal NPs catalysts.

Poly (vinyl alcohol) (PVA) as a low-cost, biocompatible and hydrophilic polymer, was usually used to prepare polymer sponge [28,29]. PVA sponge was prepared through acetalization reaction of PVA and formaldehyde using sulfuric acid as catalyst, suitable pore-forming agents and stabilizer [28]. The prepared PVA sponge exhibited excellent macroporous open-cell structure and super softness at wet state [30]. PVA sponge has been widely used as medical care pads, oil/solvent superabsorbents [31–34], support materials for the immobilization of nitrifying bacteria [35], and supporting materials for ion mining [36]. Recently, PVA has been used as a facile and elegant reducing agent for the in-situ reduction of noble metallic ions to prepare noble metal nanoparticles or noble alloy nanoparticles [37–39]. Mahanta et al. reported that the hydroxyl groups of PVA are the key functional groups responsible for the reduction of Ag-ions to AgNPs [37]. Besides, hydroxyl groups in PVA also play a key role in stabilizing AgNPs through multiple non-covalent interactions [38]. Hence, the PVA sponge is as an ideal supporting matrix to prepare and stabilize AgNPs because of reducibility, porous structure, low cost, low density and flexibility in the architectural design.

Based on the aforementioned properties of polydopamine and PVA sponge, here we report a AgNPs catalyst based on polydopamine coated polyvinyl alcohol (AgNPs/D-PVA) sponge. D-PVA sponge exhibits strong anchoring ability for AgNPs due to abundant hydroxyl and amine groups in D-PVA sponge which could be used for the in-situ fixation of Ag ions. In addition, the in-situ reduced AgNPs were stabilized through multiple non-covalent interactions between AgNPs and D-PVA sponge. AgNPs/D-PVA exhibited prominent catalytic activity for the reduction of 4-nitropehnol and can be used as a recyclable catalyst.

2. Experimental

2.1. Materials

Poly(vinyl alcohol) (PVA, polymerization degree 1750 ± 50, alcoholysis degree 98.0–99.0%), dopamine hydrochloride, TritonX-100 and 4-nitrophenol (4-NP, 99%) were purchased from Aladdin Industrial Corporation. Sulfuric acid (95–98%) was obtained from Xinyang Chemical Reagents Factory, China. Formaldehyde aqueous solution (37.0–40.0%) and silver nitrate ($AgNO_3$, 99.8%) were purchased from Sinopharm Chemical Reagent Co, Ltd, China. Sodium borohydride ($NaBH_4$, 99.0%) was purchased from Pure Sheng Fine Chemical Technology Co,Ltd, Shanghai, China. Tris(hydroxymethyl) amino methane (Tris) was obtained from Shanghai regal Biology Technology Co, Ltd, China. All the chemicals used in the experiment were analytical grade without further purification.

2.2. Preparation of PVA sponge

PVA sponge was prepared by cross-linking of PVA with formaldehyde according to the literature [40]. Firstly, a PVA solution with a concentration of 10 wt.% was obtained by dissolving 10 g of PVA in 90 g of deionized water under vigorous mechanical stirring at 90 °C [41]. And about 10 mL of formaldehyde and 1.5 g of TritonX-100 were then poured into 60 g of hot PVA solution under vigorously stirring for 5 min and a large amount of froth was observed. 30 mL of 50 wt.% H_2SO_4 was poured into the froth under vigorously stirring at room temperature for 5 min. The froth was poured into a mold and cured in an oven at 60 °C for 3 h. The raw PVA sponge was washed with water to remove the unreacted reactants. Finally, the PVA sponge was dried at 60 °C to a constant weight with an apparent density of 0.091 $g{\cdot}cm^{-3}$. The PVA sponges were cut into dimensions of 10 mm × 10 mm × 5 mm for preparing D-PVA sponges.

2.3. Preparation of AgNPs/D-PVA

Dopamine coated PVA sponges (D-PVA) were prepared as follow: PVA sponges were firstly dipped into a dopamine solution (4.0 g/L) for 10 min, and then dipped into a tris buffer solution (pH = 8.5) for the in-situ polymerization of dopamine, and finally washed with deionized water to remove unreacted dopamine and dried to constant weight at 50 °C.

D-PVA sponges were dipped into $AgNO_3$ solution (1.70×10^{-3} M) for 10 min, and then dipped into $NaBH_4$ solution (0.55 M) for 5 min, and finally was washed with deionized water and dried at 40 °C. For comparison, AgNPs/PVA was prepared with the same procedure of Ag/D-PVA except lack of dopamine participation.

2.4. Catalytic reduction of 4-NP

Catalytic reduction of 4-NP at room temperature was done according to the literature [42]. Briefly, a piece of AgNPs/PVA or AgNPs/D-PVA (60 mg) was immersed into an aqueous solution mixture of 4-NP (0.20 mM, 15 mL) and $NaBH_4$ (80.00 mM, 15 mL). The reduction of 4-NP was monitored by UV–vis spectroscopy with the scanning range of 200–500 nm. The sponge was reused after washing with water and drying.

2.5. Characterization

Fourier transform infrared (FT-IR) spectra were obtained using a FT-IR spectrometer (Nicolet 6700, USA) with attenuated total reflectance (ATR) attachment. Specific surface area, pore volume and particle size distribution of the PSM were determined by multiple point BET measurements (SA-3100, Beckman Coulter, Inc., USA). The cross-fracture morphology of the sponges was observed using a scanning electron microscope (SEM, JEOLJSM-6700F, Japan). X-ray diffraction (XRD) patterns at wide-angle (from 10° to 90° of 2θ) with Cu-K_α radiation ($\lambda = 1.54$ Å) were obtained using New D8-Advance/Bruker-AXS (Germany) powder X-ray diffractometer operating at 40 kV and 30 mA, a scanning rate of 6°/min and a scanning step of 0.02. The thermogravimetric analysis (TG) was investigated using a TA-Q5000 thermogravimetric analyzer (TA instruments, USA) at the heating rate of 10 °C/min from 30 to 700 °C under nitrogen atmosphere and 20 °C/min calefactive velocity in air flow. UV–vis spectra were carried out on a Shimadzu UV-2550 diode array spectrophotometer in a wavelength range of 200–600 nm.

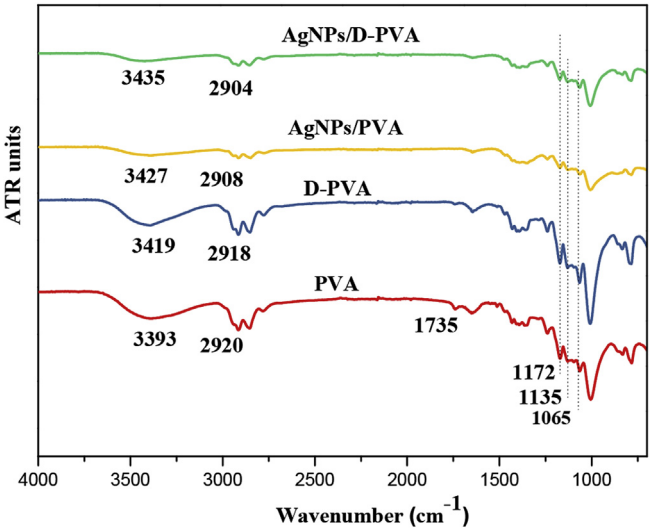

Fig. 1. FT-IR spectra of PVA (a), D-PVA (b), AgNPs/PVA (c) and AgNPs/D-PVA (d).

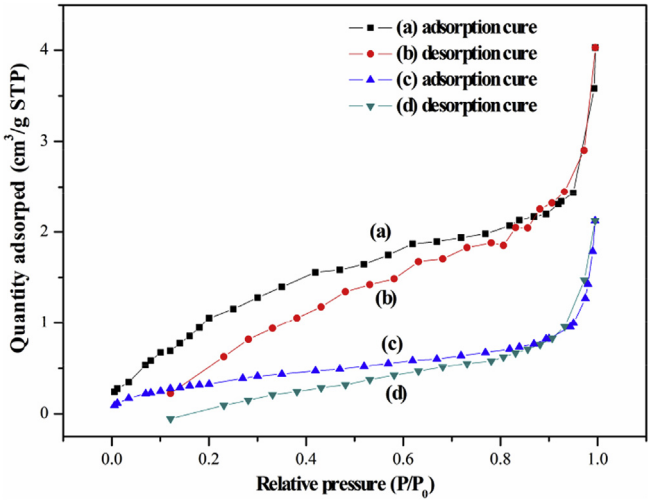

Fig. 3. Nitrogen adsorption-desorption isotherms for AgNPs/PVA (a, b) and AgNPs/D-PVA (c, d).

3. Results and discussion

3.1. Microstructure of AgNPs/D-PVA

The FT-IR spectra of PVA, D-PVA, AgNPs/PVA and AgNPs/D-PVA were shown in Fig. 1. For PVA, the broad peak at 3393 cm^{-1} is assigned to the stretching vibration of −OH. The peak at 2920, 1735 and 1007 cm^{-1} are linked to stretching vibration of C−H, C═O and C−O, respectively. Peaks at 1172, 1135 and 1065 cm^{-1} represent the C−O−C−O−C acetal structure [43], which indicates the cross-linking reaction of PVA and formaldehyde under acid condition. As for D-PVA, the absorption peaks are similar to that of PVA because of the main skeleton of PVA. Peak at 3419 cm^{-1} are deriving from hydroxyls and amines in D-PVA. The blue shifts of stretching vibration of −OH from 3393 cm^{-1} to 3419 cm^{-1} are ascribed to the intermolecular hydrogen bonding of polydopamine and PVA. Noticeably, the −OH bond of PVA and D-PVA are blue shifted from 3393 cm^{-1} and 3419 cm^{-1} to 3427 cm^{-1} and 3435 cm^{-1} after loading with AgNPs, respectively. Furthermore, the intensity of whole FT-IR spectra of AgNPs/PVA and AgNPs/D-PVA are weaken than that of the PVA and D-PVA sponge,

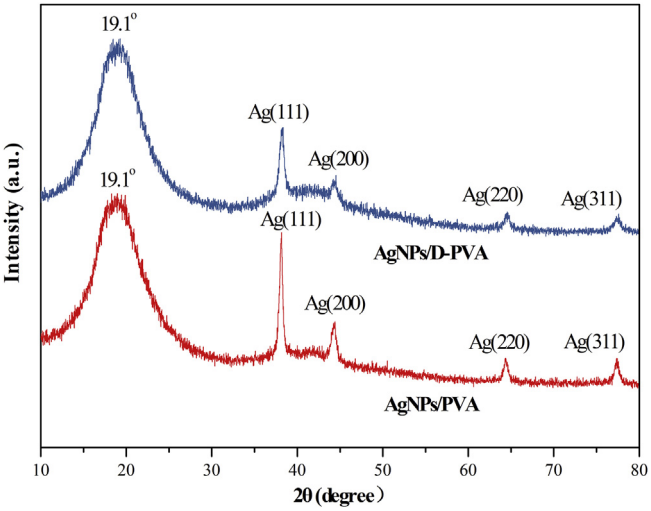

Fig. 4. XRD patterns of AgNPs/PVA and AgNPs/D-PVA.

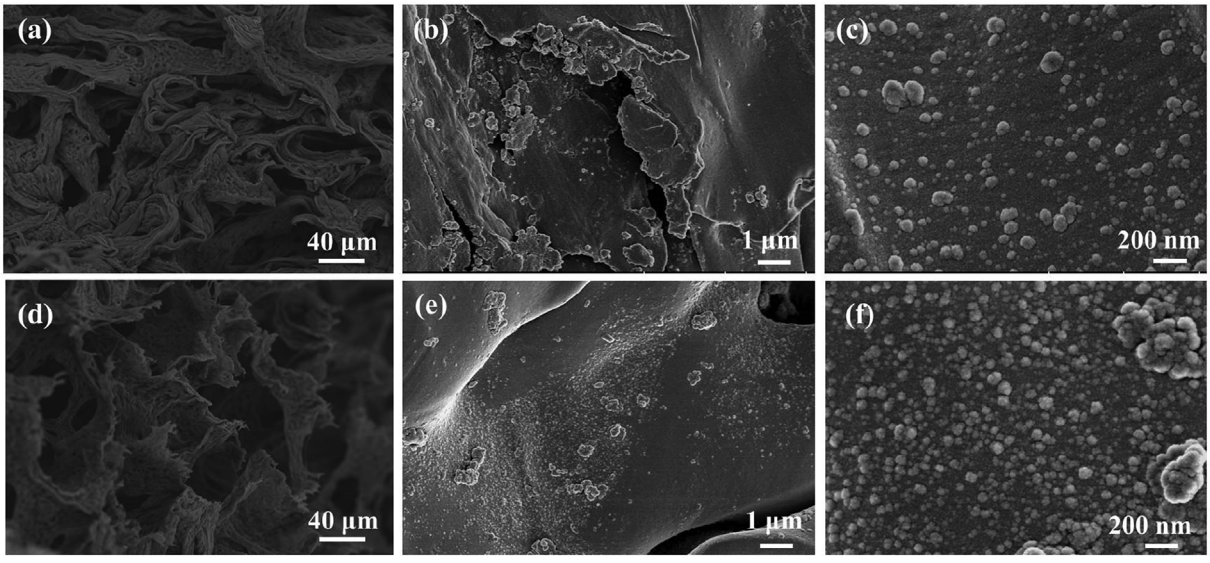

Fig. 2. SEM micrographs of PVA (a), AgNPs/PVA (b, c), D-PVA (d) and AgNPs/D-PVA (e, f).

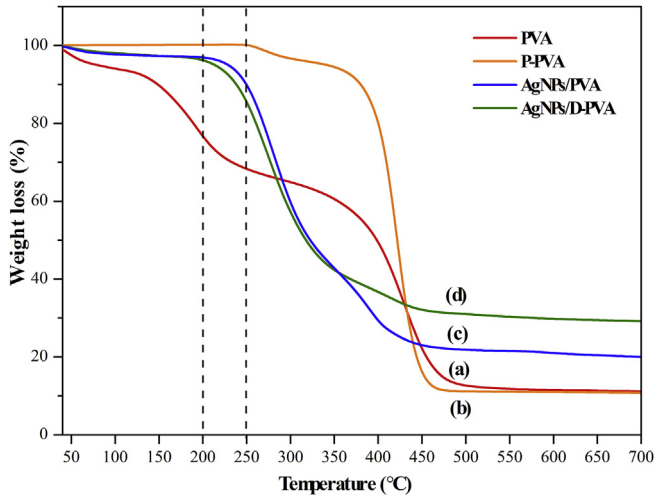

Fig. 5. TG graphs of PVA (a), D-PVA (b), AgNPs/PVA (c) and AgNPs/D-PVA (d).

respectively. This might be ascribed to the interactions between the PVA or polydopamine and the in-situ generated AgNPs [44].

The micrographs of PVA sponge (Fig. 2(a)) and D-PVA sponge (Fig. 2(d)) exhibited clear macro-porous structures, which facilitated the PVA sponge and D-PVA sponge absorbing silver ions and loading high amount of AgNPs. Fig. 2 (b, c) and Fig. 2 (e, f) showed the dimensions and distributions of AgNPs within the PVA sponge and D-PVA sponge, respectively. The average grain diameter of the AgNPs loaded on PVA sponge and D-PVA sponge is about dozens of nanometers. It noticeable that much more AgNPs were anchored on the inner wall of D-PVA sponge (Fig. 2(f)) compared to PVA sponge (Fig. 2(c)), inferring polydopamine have much stronger anchoring ability with AgNPs than that of PVA.

Nitrogen adsorption-desorption isotherms of the prepared AgNPs/PVA and AgNPs/D-PVA (Fig. 3) exhibit type II isotherm based on IUPAC classification, which indicates the macroporous characteristic of the AgNPs/PVA and AgNPs/D-PVA. The BET surface area of AgNPs/PVA and AgNPs/D-PVA was 4.9 m^2/g and 1.4 m^2/g, respectively. The reason for the low BET surface area of AgNPs/D-PVA is that polydopamine coated on the surface of PVA sponge make the specific surface areas relatively small [45]. The sorption isotherms show rise when the relative pressure P/P_0 (P is the adsorbate pressure and P_0 is the adsorbate saturated vapor pressure at the measuring temperature) is above 0.9 or 1.0, revealing the existence of macro-pores [46], which is in agreement with the SEM results.

The XRD patterns of the AgNPs/PVA and AgNPs/D-PVA samples were shown in Fig. 4. The peak at 19.1° is consistent with the (101) diffraction peak of pure PVA as a semi-crystalline polymer [47]. Four

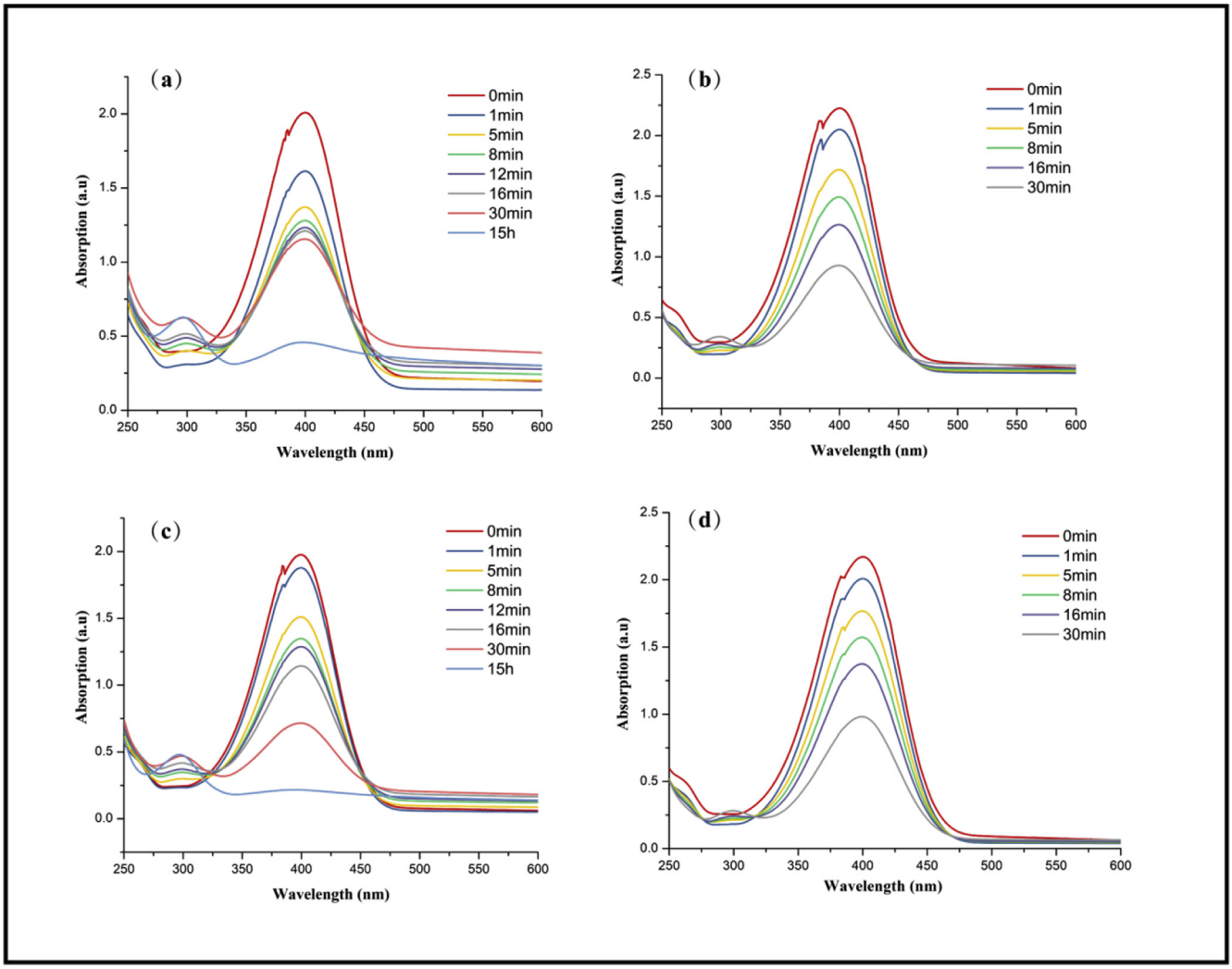

Fig. 6. UV–vis spectra of the aqueous 4-NP solution (initial concentration = 0.10×10^{-3} M). (a) the first catalysis of AgNPs/PVA; (b) the fourth catalysis AgNPs/PVA; (c) the first catalysis AgNPs/D-PVA; (d) the fourth catalysis AgNPs/D-PVA.

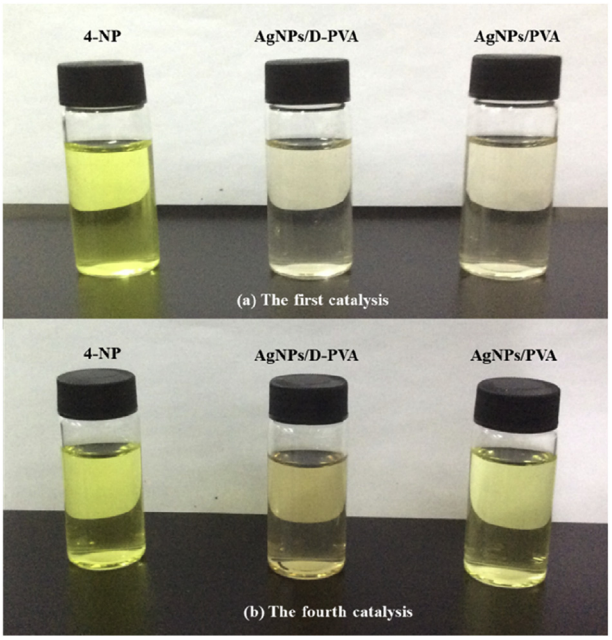

Fig. 7. Photographs of the 4-NP solution taken before and after first (a) and fourth (b) catalysis by AgNPs/PVA and AgNPs/D-PVA.

sharp diffraction peaks appeared at 2θ = 38.2°, 44.4°, 64.4° and 77.4° for AgNPs/PVA sponge and 2θ = 38.4°, 44.6°, 64.7° and 77.6° for AgNPs/D-PVA sponge can be indexed to the (111), (200), (220) and (311) planes of pure face centered cubic (fcc) Ag crystals, respectively [42,48,49]. This is consistent with the standard value according to JCPDS Card no.04–0783. The deviation of the 2θ is caused by different sizes of AgNPs of AgNPs/PVA and AgNPs/D-PVA. The result of XRD displays that Ag ions have been successfully converted to metallic Ag by the reduction [4,17]. The crystallite size of AgNPs were calculated using the Debye-Scherrer equation with $d_{XRD} = 0.89\lambda/\beta\cos\theta$, where d_{XRD} is the crystallite size, λ is the wavelength of x-ray used (λ = 1.54 Å), and θ and β are the half diffraction angle (2θ) and full width at half maximum of the XRD intensity lines, respectively. The strongest (111) was taken to calculate the crystallite size of AgNPs of AgNPs/PVA and AgNPs/D-PVA and the results are about 15.6 nm and 10.2 nm for AgNPs/PVA and AgNPs/D-PVA, respectively. Due to strong coordination interaction between silver ions and catechol groups of polydopamine layer, AgNPs with uniform structure and nanoscale size can be synthesized and in situ anchored in one step [50]. Therefore, the crystallite size of AgNPs of AgNPs/D-PVA is smaller than that of AgNPs/PVA.

Thermal stability of PVA, D-PVA, AgNPs/PVA and AgNPs/D-PVA was evaluated by TG analysis and the results are shown in Fig. 5. For pure PVA, there are mainly three weight-loss stages below 100 °C, 100–250 °C and 250–450 °C (Fig. 5(a)), in which the first weight-loss of 10% corresponds to the evaporation of physically adsorbed water, the second weight loss of about 30% is due to the dehydration of PVA molecular chain and the third weight loss of about 50% is due to the main chain scissions of PVA. When PVA was coated with polydopamine, an obvious increase in thermal stability of D-PVA compared to PVA as evidenced by a large shifting of the onset temperature decomposition from 100 °C to 250 °C, which is consistent with the fact that PDA modified composites usually exhibit excellent high thermal stability [25,51,52]. This phenomenon might be due to the reason that the PDA can be tightly adhered to the surface of PVA sponge and form strong non-covalent interaction with PVA [51]. The decomposition behavior of D-PVA is similar to that of pure PDA at 200–500 °C stage [53]. The weight-loss of AgNPs/PVA and AgNPs/D-PVA were serious compared with that of PVA sponge and D-PVA sponge between 300 and 450 °C. The reason might be that AgNPs have good heat conducting properties, which make PVA and D-PVA sponge susceptible to heat and reduce the initial decomposition temperature of AgNPs/PVA and AgNPs/D-PVA. Compared with the weight loss curves of PVA and AgNPs/PVA, the initial decomposition temperature of AgNPs/PVA was increased about 200 °C and the amount of residual Ag was about 10 wt.%. Compared with D-PVA sponge, the initial decomposition temperature of AgNPs/D-PVA was reduced by 50 °C and the amount of residual Ag was about 20 wt.%. Higher amount of AgNPs in AgNPs/D-PVA was attributed to more Ag ions anchored sites of D-PVA when compared with that of PVA.

3.2. Catalytic properties

4-nitrophenol (4-NP) is a common toxic pollutant in industrial waste water, which is harmful to human and animals. However, 4-aminophenol (4-AP), the reduction form of 4-NP, is a useful industrial precursor with various application in dyeing agent and corrosion inhibitors [54–56]. Nevertheless, the catalysis degradation of 4-NP by

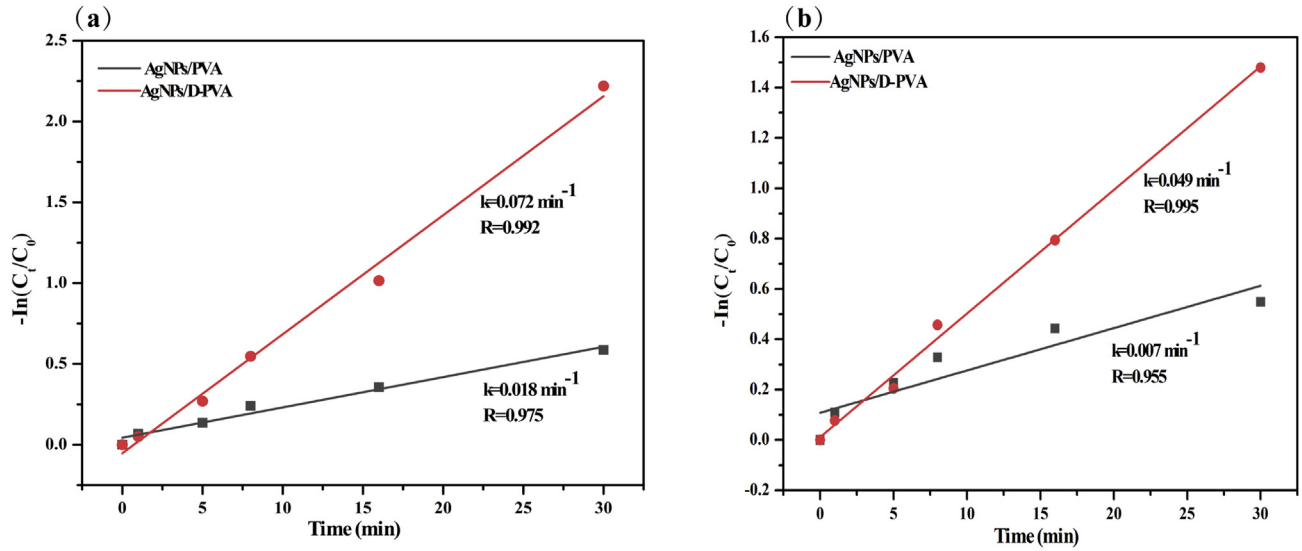

Fig. 8. Plots of $-\ln(C_t/C_0)$ versus time during the catalytic reduction of 4-NP by AgNPs/PVA and AgNPs/D-PVA. (a) the first catalysis of AgNPs/PVA and AgNPs/D-PVA; (b) the fourth catalysis AgNPs/PVA and AgNPs/D-PVA.

Table 1
Comparison of catalytic activity of AgNPs/polymer catalysts synthesized using different methods towards the reduction of 4-NP.

AgNPs/polymer catalysts	Support	Concentration of $AgNO_3$ solution used for the immersion of support (mmol/L)	Rate constant of catalyst [min^{-1}]	Ref.
AgNPs/polyacrylamide/polypyrrole/graphene oxide	Polyacrylamide/polypyrrole/graphene oxide	17.6	1.98	[15]
AgNPs/cellulose paper	Cellulose paper	10.0	0.88	[16]
S-MOPS-Ag	Microporous organic polymer (MOP) sponge	18.2	0.46	[40]
AgNPs/D-PVA	D-PVA sponge	1.7	0.072	This work

traditional methods are usually ineffective due to high stability and low solubility of 4-NP in water. For this reason, there is a great demand for direct catalytic reduction of 4-NP to 4-AP. The reduction of 4-NP over AgNPs in the presence of $NaBH_4$ is an efficient and eco-friendly route to produce 4-AP [42]. Here, the reduction of 4-NP to 4-AP with excess $NaBH_4$ was selected as a model reaction to evaluate the catalytic properties AgNPs/D-PVA.

A reaction yellow green solution was prepared by mixing aqueous 4-NP and $NaBH_4$ which showed an absorption maximum around 400 nm due to the formation of 4-nitrophenolate ion at the alkaline conditions [14]. For the catalytic reaction to proceed, AgNPs/PVA and AgNPs/D-PVA were immersed in the reaction solution via vigorous agitation. After addition of AgNPs/PVA or AgNPs/D-PVA, the absorption peak intensity of 4-NP at 400 nm was gradually reduced and a new absorption peak of 4-AP was appeared and enhanced around 300 nm (see Fig. 6). After 30 min, the initially yellow green solution turned almost light yellow or colorless (Fig. 7), suggesting the near completion of the reduction reaction.

According to references [17,42], the pseudo first-order kinetic equation was used to describe the overall reaction as follows:

$$\mathrm{In}(C_t/C_0) = -kt \quad (1)$$

Where C_t is the concentration of 4-NP at reaction time t, and C_0 is the initial concentration [42]. It can be seen from Fig. 8 that the reactions showed linear correlation between $\mathrm{In}(C_t/C_0)$ and time. The apparent rate constant of the first catalytic reaction with AgNPs/D-PVA was 0.072 min^{-1}, which was higher than that of AgNPs/PVA. Besides, the apparent rate constant of the fourth catalytic reaction with AgNPs/D-PVA was 0.049 min^{-1}, indicating that AgNPs/D-PVA maintains excellent catalytic properties for 4-NP in recirculation. Hence, it can be concluded that polydopamine played a significant role in improving the catalytic performance of AgNPs/PVA. In addition, both AgNPs/PVA and AgNPs/D-PVA can be easily removed from the reaction mixture and reused after washing and drying. The good stability and reusability could result from the efficient anchoring of AgNPs on the inner-wall of D-PVA sponges. When compared with AgNPs synthesized by other procedures, the present reported AgNPs supported by D-PVA sponges possessed comparable catalytic performance (Table 1). The relative smaller rate constant of AgNPs/D-PVA was due to low $AgNO_3$ solution used for the immersion of D-PVA shown in Table 1.

A schematic representation of the preparation of AgNPs/PVA and AgNPs/D-PVA was proposed and illuminated in Fig. 9. As shown, the prepared PVA sponge contained abundant hydroxyl groups and D-PVA sponge contained abundant hydroxyl groups and amino groups. The electron-rich oxygen atoms and nitrogen atoms are able to combine with the Ag ions due to strong electrostatic interactions leading to immobilization of Ag ions and the Ag ions were kept stable and uniformly distributed on the surfaces of PVA sponge and D-PVA sponge. When the PVA sponge and D-PVA sponge with Ag ions were immersed in the aqueous solution of $NaBH_4$, the Ag ions were quickly reduced to AgNPs. Meanwhile, owing to being tightly anchored by the hydroxyl and amino groups, the reduced AgNPs were stabilized at the original ionized selective sites on the surfaces of PVA sponge and D-PVA sponge, which avoids the aggregation of AgNPs resulting in excellent dispersion effect [57]. Liang et al. reported that amino groups on the surface of cellulose paper can provide stable anchoring centers for silver ions [17]. Therefore, the D-PVA sponge containing amino groups possesses better Ag ions fixation capacity than that of PVA sponge, which is proved by the results of SEM, TG and UV–vis analysis.

4. Conclusions

In summary, AgNPs/D-PVA catalyst was successfully prepared and was used to hydrogenation reduction of highly toxic 4-NP. The D-PVA sponge possesses better Ag ions fixation capacity and AgNPs anchoring

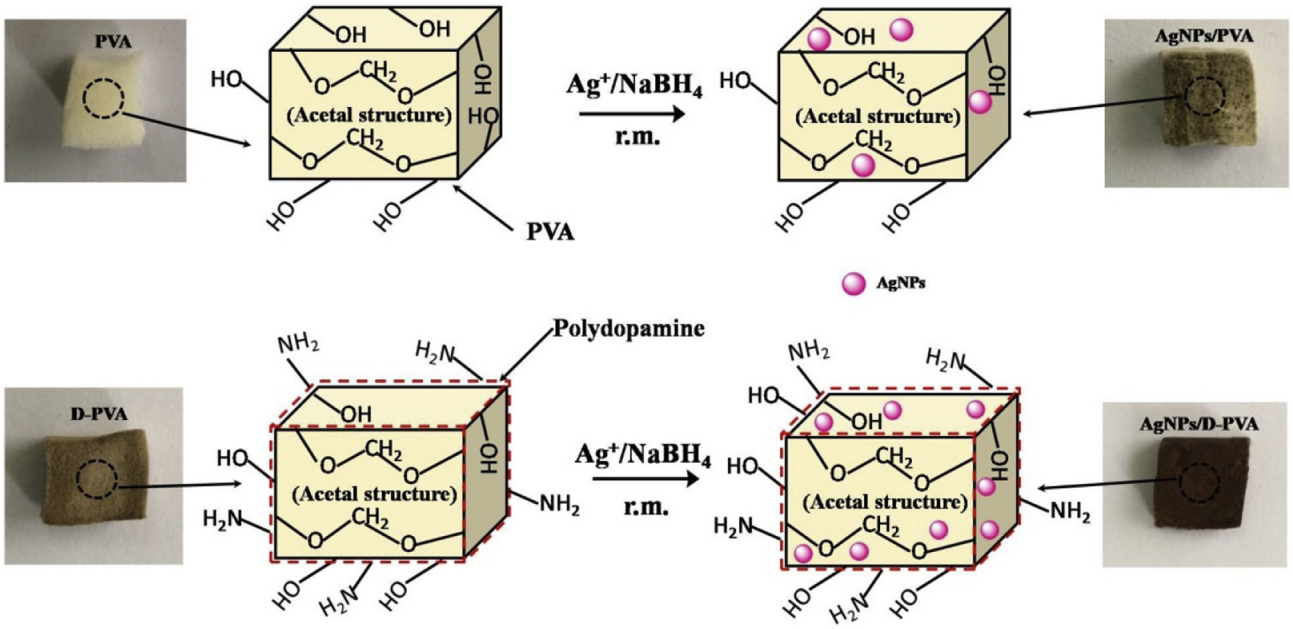

Fig. 9. Schematic representation of the preparation of AgNPs/PVA and AgNPs/D-PVA.

ability than that of PVA sponge due to abundant anchoring sites such as hydroxyl groups and amino groups, which is proved by the results of FTIR, SEM and TG analysis. AgNPs/D-PVA exhibited better catalytic activity during four cycles when compared with AgNPs/PVA. By combining the merits of dopamine modification and PVA sponge, this work provided a strategy to develop low cost and high performance of 4-nitrophenol nanocatalyst.

Acknowledgements

This work was supported by the Natural National Science Foundation of China (51373126). The authors also appreciate the fund support of Wuhan Institute of Technology, China (Q201701 and 2017031).

Appendix A. Supplementary data

Supplementary data to this article can be found online at https://doi.org/10.1016/j.matchemphys.2018.12.049.

Conflicts of interest

The authors declare that they have no conflicts of interest. The authors alone are responsible for the content and writing of this article.

References

[1] Y.Q. Zhao, J. Feng, L. Hong, Y.X. Li, C.X. Wang, S.J. Ye, Simple surface-assisted formation of palladium nanoparticles on polystyrene microspheres and their application in catalysis, Inorg. Chem. Front. 5 (2018) 1133–1138.
[2] S.U. Rehman, A.R. Khan, A. Shah, A. Badshah, M. Siddiq, Preparation and characterization of poly(N-isoproylacrylamide-co-dimethylaminoethyl methacrylate) microgels and their composites of gold nanoparticles, Colloid. Surface. 520 (2017) 826–833.
[3] Y. Meng, L.Q. Cai, X.J. Xu, L.N. Zhang, Construction of size-controllable gold nanoparticles immobilized on polysaccharide nanotubes by in situ one-pot synthesis, Int. J. Biol. Macromol. 113 (2018) 240–247.
[4] Z.L. Yan, L.J. Fu, X.C. Zuo, H.M. Yang, Green assembly of stable and uniform silver nanoparticles on 2D silica nanosheets for catalytic reduction of 4-nitrophenol, Appl. Catal. B Environ. 226 (2018) 23–30.
[5] G.F. Liao, Q. Li, W.Z. Zhao, Q.H. Pang, H.Y. Gao, Z.S. Xu, In-situ construction of novel silver nanoparticle decorated polymeric spheres as highly active and stable catalysts for reduction of methylene blue dye, Appl. Catal. A-Gen. 549 (2018) 102–111.
[6] G.F. Liao, J. Chen, W.G. Zeng, C.H. Yu, C.F. Yi, Z.S. Xu, Facile preparation of uniform nanocomposite spheres with loading silver nanoparticles on polystyrene-methyl acrylic acid spheres for catalytic reduction of 4-nitrophenol, J. Phys. Chem. C 120 (2016) 25935–25944.
[7] Z. Yan, L. Fu, X. Zuo, H. Yang, Green assembly of stable and uniform silver nanoparticles on 2D silica nanosheets for catalytic reduction of 4-nitrophenol, Appl. Catal. B Environ. 226 (2018) 23–30.
[8] S.M. Sadeghzadeh, R. Zhiani, S. Emrani, A versatile supported silver for heterogeneously catalysed processes: synthesis of 3-acyloxylindolines solvent-free conditions, Appl. Organomet. Chem. 32 (2018) e4130.
[9] H. Heidari, Ag nanoparticle/nanofibrillated cellulose composite as an effective and green catalyst for reduction of 4-nitrophenol, J. Cluster Sci. 29 (2018) 475–481.
[10] Z. Lu, J.T. Gao, Q.F. He, J. Wu, D.H. Liang, H. Yang, R. Chen, Enhanced antibacterial and wound healing activities of microporous chitosan-Ag/ZnO composite dressing, Carbohydr. Polym. 156 (2017) 460–469.
[11] D. Liang, Z. Lu, H. Yang, J. Gao, R. Chen, Novel asymmetric wettable Agnps/chitosan wound dressing: in vitro and in vivo evaluation, Acs Appl. Mater. Inter. 8 (2016) 3958–3968.
[12] Z. Lu, J. Gao, Q. He, J. Wu, D. Liang, H. Yang, R. Chen, Enhanced antibacterial and wound healing activities of microporous chitosan-Ag/ZnO composite dressing, Carbohydr. Polym. 156 (2017) 460–469.
[13] X.D. Guo, G.L. Liu, S. Yue, J. He, L.Y. Wang, Hydroxyl-rich nanoporous carbon nanosheets synthesized by a one-pot method and their application in the in situ preparation of well-dispersed Ag nanoparticles, RSC Adv. 5 (2015) 96062–96066.
[14] X.H. Zhao, Q. Li, X.M. Ma, Z. Xiong, F.Y. Quan, Y.Z. Xia, Alginate fibers embedded with silver nanoparticles as efficient catalysts for reduction of 4-nitrophenol, RSC Adv. 5 (2015) 49534–49540.
[15] S.M. Alshehri, T. Almuqati, N. Almuqati, E. Al-Farraj, N. Alhokbany, T. Ahamad, Chitosan based polymer matrix with silver nanoparticles decorated multiwalled carbon nanotubes for catalytic reduction of 4-nitrophenol, Carbohydr. Polym. 151 (2016) 135–143.
[16] H. Mao, C. Ji, M. Liu, Z. Cao, D. Sun, Z. Xing, X. Chen, Y. Zhang, X.M. Song, Enhanced catalytic activity of Ag nanoparticles supported on polyacrylamide/polypyrrole/graphene oxide nanosheets for the reduction of 4-nitrophenol, Appl. Surf. Sci. 434 (2018) 522–533.
[17] M. Liang, G. Zhang, Y. Feng, R. Li, P. Hou, J. Zhang, J. Wang, Facile synthesis of silver nanoparticles on amino-modified cellulose paper and their catalytic properties, J. Mater. Sci. 53 (2018) 1568–1579.
[18] H. Lee, S.M. Dellatore, W.M. Miller, P.B. Messersmith, Mussel-inspired surface chemistry for multifunctional coatings, Science 318 (2007) 426–430.
[19] Y. Ni, G. Tong, J. Wang, H. Li, F. Chen, C. Yu, Y. Zhou, One-pot preparation of pomegranate-like polydopamine stabilized small gold nanoparticles with superior stability for recyclable nanocatalysts, RSC Adv. 6 (2016) 40698–40705.
[20] S.N. Du, Y. Luo, Z.F. Liao, W. Zhang, X.H. Li, T.Y. Liang, F. Zuo, K.Y. Ding, New insights into the formation mechanism of gold nanoparticles using dopamine as a reducing agent, J. Colloid Interface Sci. 523 (2018) 27–34.
[21] S. Peng, F. Gao, D. Zeng, C. Peng, Y. Chen, M. Li, Synthesis of Ag-Fe_3O_4 nanoparticles supported on polydopamine-functionalized porous cellulose acetate microspheres: catalytic and antibacterial applications, Cellulose 25 (2018) 4771–4782.
[22] W. Xiong, X. Li, Q. Zhao, Y. Shi, C. Hao, Insight into the photocatalytic mineralization of short chain chlorinated paraffins boosted by polydopamine and Ag nanoparticles, J. Hazard Mater. 359 (2018) 186–193.

[23] K. Cui, B. Yan, Y. Xie, H. Qian, X. Wang, Q. Huang, Y. He, S. Jin, H. Zeng, Regenerable urchin-like Fe_3O_4@PDA-Ag hollow microspheres as catalyst and adsorbent for enhanced removal of organic dyes, J. Hazard Mater. 350 (2018) 66–75.
[24] G. Su, C. Yang, J.J. Zhu, Fabrication of gold nanorods with tunable longitudinal surface plasmon resonance peaks by reductive dopamine, Langmuir 31 (2015) 817–823.
[25] F. Luo, K. Wu, J. Shi, X. Du, X. Li, L. Yang, M. Lu, Green reduction of graphene oxide by polydopamine to a construct flexible film: superior flame retardancy and high thermal conductivity, J. Mater. Chem. 5 (2017) 18542–18550.
[26] J. Zhou, B. Duan, Z. Fang, J. Song, C. Wang, P.B. Messersmith, H. Duan, Interfacial assembly of mussel-inspired Au@Ag@polydopamine core-shell nanoparticles for recyclable nanocatalysts, Adv. Mater. 26 (2014) 701–705.
[27] Y. Liu, K. Ai, L. Lu, Polydopamine and its derivative materials: synthesis and promising applications in energy, environmental, and biomedical fields, Chem. Rev. 114 (2014) 5057–5115.
[28] Y.I. Chang, Y.Y. Yang, W.Y. Cheng, L. Jang, Making PVF porous sponge with and without using the pore-forming agent-A comparison, J. Taiwan Inst. Chem. E. 74 (2017) 246–254.
[29] Y.I. Chang, J.W. Chen, W.Y. Cheng, L. Jang, The reinforcement of the physical strength of PVA sponge through the double acetalization, Separ. Purif. Technol. 198 (2018) 100–107.
[30] R. Nishiyabu, S. Iizuka, S. Minegishi, H. Kitagishi, Y. Kubo, Surface modification of a polyvinyl alcohol sponge with functionalized boronic acids to develop porous materials for multicolor emission, chemical sensing and 3D cell culture, Chem. Commun. 53 (2017) 3563–3566.
[31] Y.X. Pan, K. Shi, C. Peng, W.C. Wang, Z. Liu, X.L. Ji, Evaluation of hydrophobic polyvinyl-alcohol formaldehyde sponges as absorbents for oil spill, Acs Appl. Mater. Inter. 6 (2014) 8651–8659.
[32] C.P. Su, H. Yang, H.P. Zhao, Y.L. Liu, R. Chen, Recyclable and biodegradable superhydrophobic and superoleophilic chitosan sponge for the effective removal of oily pollutants from water, Chem. Eng. J. 330 (2017) 423–432.
[33] C.P. Su, H. Yang, S. Song, B. Lu, R. Chen, A magnetic superhydrophilic/oleophobic sponge for continuous oil-water separation, Chem. Eng. J. 309 (2017) 366–373.
[34] S. Song, H. Yang, C.P. Su, Z.B. Jiang, Z. Lu, Ultrasonic-microwave assisted synthesis of stable reduced graphene oxide modified melamine foam with superhydrophobicity and high oil adsorption capacities, Chem. Eng. J. 306 (2016) 504–511.
[35] H. Bae, H. Yang, Y.C. Chung, Y. Yoo, S. Lee, High-rate partial nitritation using porous poly(vinyl alcohol) sponge, Bioproc. Biosyst. Eng. 37 (2014) 1115–1125.
[36] L.A. Limjuco, G.M. Nisola, C.P. Lawagon, S.P. Lee, J.G. Seo, H. Kim, W.J. Chung, H_2TiO_3 composite adsorbent foam for efficient and continuous recovery of Li^+ from liquid resources, Colloid. Surface. 504 (2016) 267–279.
[37] N. Mahanta, S. Valiyaveettil, In situ preparation of silver nanoparticles on biocompatible methacrylated poly(vinyl alcohol) and cellulose based polymeric nanofibers, RSC Adv. 2 (2012) 11389–11396.
[38] A. Kyrychenko, D.A. Pasko, O.N. Kalugin, Poly(vinyl alcohol) as a water protecting agent for silver nanoparticles: the role of polymer size and structure, Phys. Chem. Chem. Phys. 19 (2017) 8742–8756.
[39] V.K. Rao, T.P. Radhakrishnan, Tuning the SERS response with Ag-Au nanoparticle-embedded polymer thin film substrates, Acs Appl. Mater. Inter. 7 (2015) 12767–12773.
[40] Y. Pan, W. Wang, C. Peng, K. Shi, Y. Luo, X. Ji, Novel hydrophobic polyvinyl alcohol-formaldehyde foams for organic solvents absorption and effective separation, RSC Adv. 4 (2014) 660–669.
[41] F.P. Du, E.Z. Ye, W. Yang, T.H. Shen, C.Y. Tang, X.L. Xie, X.P. Zhou, W.C. Law, Electroactive shape memory polymer based on optimized multi-walled carbon nanotubes/polyvinyl alcohol nanocomposites, Compos. B Eng. 68 (2015) 170–175.
[42] J.G. Kim, M.C. Cha, J. Lee, T. Choi, J.Y. Chang, Preparation of a sulfur-functionalized microporous polymer sponge and in situ growth of silver nanoparticles: a compressible monolithic catalyst, Acs Appl. Mater. Inter. 9 (2017) 38081–38088.
[43] H.Y. Guan, F. Lian, K. Xi, Y. Ren, J.L. Sun, R.V. Kumar, Polyvinyl formal based gel polymer electrolyte prepared using initiator free in-situ thermal polymerization method, J. Power Sources 245 (2014) 95–100.
[44] J.B. Campos, E. Prokhorov, I.C. Sanchez, J.G. Barcenas, A.M. Ramirez, J.G. Hernandez, Y.L. Castro, R.E. Rio, Molecular dynamics analysis of PVA-AgNP composites by dielectric spectroscopy, J. Nanomater. 2012 (2012) 925750.
[45] W. Cheng, C.Y. Liang, L. Xu, G. Liu, N.S. Gao, W. Tao, L.Y. Luo, Y.X. Zuo, X.S. Wang, X.D. Zhang, X.W. Zeng, L. Mei, TPGS-functionalized polydopamine-modified mesoporous silica as drug nanocarriers for enhanced lung cancer chemotherapy against multidrug resistance, Small 13 (2017) 1700623.
[46] M.U. Sheikh, G.A. Naikoo, M. Thomas, M. Bano, F. Khan, Surfactant-assisted morphological tuning of porous metallic silver sponges: facile synthesis, characterization and catalytic performance, J. Sol. Gel Sci. Technol. 76 (2015) 572–581.
[47] S. Ma, J.J. Hou, H. Yang, Z.L. Xu, Preparation of renewable porous TiO_2/PVA composite sphere as photocatalyst for methyl orange degradation, J. Porous Mater. 25 (2018) 1071–1080.
[48] Y. Mao, J. Wei, C. Wang, Y. Feng, H. Yang, X. Meng, Growth and characterization of sponge-like silver with high catalytic activity for the reduction of p-nitrophenol, Mater. Lett. 154 (2015) 47–50.
[49] M. Bano, D. Ahirwar, M. Thomas, G.A. Naikoo, M.U. Sheikh, F. Khan, Hierarchical synthesis of silver monoliths and their efficient catalytic activity for the reduction of 4-nitrophenol to 4-aminophenol, New J. Chem. 40 (2016) 6787–6795.
[50] X.M. Wang, W. Zhou, C.L. Wang, Z.L. Chen, In situ immobilization of layered double hydroxides onto cotton fiber for solid phase extraction of fluoroquinolone drugs, Talanta 186 (2018) 545–553.
[51] Y. Liao, M. Wang, D. Chen, Preparation of polydopamine-modified graphene oxide/chitosan aerogel for uranium (VI) adsorption, Ind. Eng. Chem. Res. 57 (2018) 8472–8483.
[52] J.Y. Lin, Z.X. Yang, X.X. Hu, G.H. Hong, S.B. Zhang, W. Song, The effect of alkali treatment on properties of dopamine modification of bamboo fiber/polylactic acid composites, Polymers-basel 10 (2018) 403.
[53] A.S. Subramanian, J.N. Tey, L. Zhang, B.H. Ng, S. Roy, J. Wei, X.M. Hu, Synergistic bond strengthening in epoxy adhesives using polydopamine/MWCNT hybrids, Polymer 82 (2016) 285–294.
[54] H.W. Hu, J.H. Xin, H. Hu, PAM/graphene/Ag ternary hydrogel: synthesis, characterization and catalytic application, J. Mater. Chem. 2 (2014) 11319–11333.
[55] Y.Z. Li, Y.L. Cao, J. Xie, D.Z. Jia, H.Y. Qin, Z.T. Liang, Facile solid-state synthesis of Ag/graphene oxide nanocomposites as highly active and stable catalyst for the reduction of 4-nitrophenol, Catal. Commun. 58 (2015) 21–25.
[56] X. Zhang, H. Xiang, Q. Wang, H. Cao, J. Xue, Carbon encapsulated $FeCu_4$ alloy nanoparticles modified glass carbon electrode to promote the degradation for p-nitrophenol, Integrated Ferroelectrics Int. J. 147 (2013) 97–102.
[57] C. Wan, Y. Jiao, Q. Sun, J. Li, Preparation, Characterization, and antibacterial properties of silver nanoparticles embedded into cellulose aerogels, Polym. Compos. 37 (2016) 1137–1142.